

Log-domain All-pass Filter-based Multiphase Sinusoidal Oscillators

Pipat PROMMEE, Natapong WONGPROMMOON

Dept. of Telecommunication Engineering, Faculty of Engineering, King Mongkut's Inst. of Technology Ladkrabang, Bangkok 10520, Thailand

pipat@telecom.kmitl.ac.th

Abstract. *Log-domain current-mode multiphase sinusoidal oscillators based on all-pass filters are presented in this paper. The first-order differential equation is used for obtaining inverting and non-inverting all-pass filters. The proposed oscillators are realized by all-pass filters whose natural frequency and stage gain can be electronically tuned by adjusting the bias currents. Each all pass filter contains 10 NPN transistors and a grounded capacitor. The validated BJT model which is used in SPICE simulation operated by a single power supply as low as 2.5 V. The frequency of oscillation can be controlled over four decades. The total harmonic distortions of these MSO at frequency 56.67 MHz and 54.44 MHz, obtained around 0.52% and 0.75%, respectively. The proposed circuits enable fully integrated in telecommunication systems and also suit to high-frequency applications. Nonideality studies and PSpice simulation results are included to confirm the theory.*

Keywords

All-pass filter, log-domain filtering, high-frequency, low-voltage, electronically-controlled, multiphase sinusoidal oscillator.

1. Introduction

Log-domain circuits are useful building blocks for realizing high-performance current-mode analogue signal processing systems. In 1979, Adams introduced a novel class of continuous-time filters called log-domain filters which externally are linear systems, yet internally are nonlinear [1]. The proposed circuit is originated from the companding concept of log-domain circuits. Input linear current is initially converted to a compressed voltage. Compressed voltage is processed by the log-domain core block. The compressed output voltage is converted to a linear current to preserve the linear operation of the whole system. The compression and expansion of the corresponding signals are based on the logarithmic/exponential voltage-current relationship of a bipolar transistor.

In 1993, Frey introduced a general method for synthesizing log-domain filters of arbitrary order using a state-space approach [2], [3]. Frey also presented a highly modular technique for implementing such filters from a simple building block comprising a bipolar current mirror whose emitters are driven by complementary emitter followers. Log-domain filter operations are based on instantaneous companding [4]–[7] and these previous circuits are of theoretical and technological interest because they potentially offer high-frequency operation, tunability, and extended dynamic range under low power supply voltages [8]–[14]. Log-domain circuits based on CMOS technology were introduced [15] which need to bias in weak inversion region. Complexity and low-bandwidth are the drawback of this circuit.

Multiphase Sinusoidal Oscillator (MSO) is appropriate to use in many applications. For example, in telecommunications MSO is used in realizing phase modulator, quadrature mixers and single-sideband generators. For measurement purposes, MSO is used in realizing vector generators or selective voltmeters. Moreover, MSO constitutes an important unit in many communication and instrumentation systems [26]. Current-conveyors with grounded capacitors [16], [17] were used in MSO realization. OTAs and grounded capacitors were also introduced to use in realization of MSO and a third-order oscillator [18]. OPAMP with RC components [19], current-differencing transconductance amplifiers (CDTA) with floating capacitors [20] and current-controlled current-differencing transconductance amplifiers (CCCDTA) with grounded capacitors [21] are introduced to use in MSO based on the all-pass (AP) sections. The previous MSOs suit to IC production, but not to high-frequency operations. Log-domain MSO [22] and quadrature sinusoidal oscillator (QSO) [23] are also proposed including the following potential capabilities: low-voltage, high-frequency and wide electronic tuning. The circuit uses synthesis method of exponential and log cells, hence it suffers from high complexity and a high number of transistors per phase.

Low-complexity log-domain MSO and QSO have been introduced based on LP filter [24] and lossless integrator [25], respectively. Since 2012, log-domain MSO based on only inverting AP filter has been introduced [26].

$$I_1 I_2 = I_{C3} I_O. \tag{10}$$

The collector current of Q_3 can be expressed as

$$I_{C3} = I_3 + C_1 \dot{V}_{C1}. \tag{11}$$

The derivative of the voltage across the capacitor C_1 is

$$\dot{V}_{C1} = \frac{dV_{C1}}{dt} = \frac{V_T}{I_O} \frac{dI_O}{dt} = \frac{V_T \dot{I}_O}{I_O} \tag{12}$$

where $I_O = I_S \exp(V_{C1}/V_T)$, the derivative of the output current yields

$$\dot{I}_O = \frac{dI_O}{dt} = \frac{I_O}{V_T} \dot{V}_{C1} = \frac{I_S}{V_T} \exp\left(\frac{V_{C1}}{V_T}\right) \frac{dV_{C1}}{dt}. \tag{13}$$

Substituting (11), (12) and (13) into (10), we get

$$I_1 I_2 = \left(I_3 + \frac{C_1 V_T \dot{I}_O}{I_O} \right) I_O. \tag{14}$$

Suppose we define the currents $I_2 = kI_3 = kI$; then equation (14) becomes

$$kI_1 = I_O + \frac{C_1 V_T \dot{I}_O}{I}. \tag{15}$$

By taking the Laplace transform of (15) and rearranging, the transfer function of the circuit in Fig. 3(a) is given by

$$H(s) = \frac{I_O(s)}{I_1(s)} = \frac{k}{s(C_1 V_T / I) + 1}. \tag{16}$$

From (16), where $k = I_2/I_3$ and $V_T = 26$ mV at room temperature, it can be seen that $H(s)$ corresponds to the transfer function of a LP filter. The natural frequency is controlled by the bias current (I).

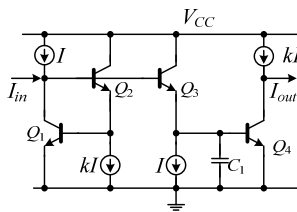


Fig. 4. Inverting log-domain LP filter [24].

From Fig. 3, if the currents I_1 , I_2 , and I_3 are, respectively, replaced by $I_1 = I + I_{in}$, $I_2 = kI$ and $I_3 = I$. A current source kI will be inserted at the output for cancelling the DC-offset. Then Fig. 3 is transformed to Fig. 4 [24]. The current output of completed inverting log-domain low-pass filter is obtained in s -domain function as

$$\frac{I_{out}(s)}{I_{in}(s)} = \frac{-k}{s(C_1 V_T / I) + 1}. \tag{17}$$

Fig. 5(a) shows the block diagram of the proposed AP filter realized from a LP filter. The AP filter consists of

a LP filter, two amplifiers (gain = 2 and gain = k) and a summing junction. Then the inverting AP filter transfer function of Fig. 5(a) can be written as

$$\frac{Y(s)}{X(s)} = k \left(\frac{sA - 1}{sA + 1} \right). \tag{18}$$

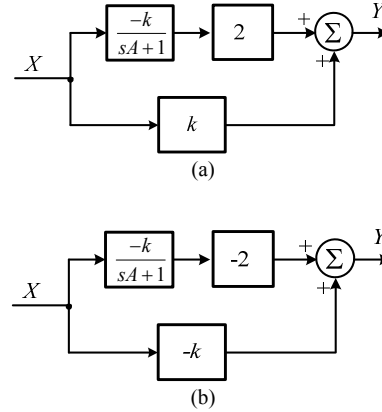


Fig. 5. AP filter realized by LP filter block diagram: (a) Inverting, (b) Non-inverting.

Considering Fig. 5(b), the non-inverting AP filter can be obtained by assigning the both amplifier blocks to negative. The non-inverting AP filter transfer function can be written as

$$\frac{Y(s)}{X(s)} = k \left(\frac{1 - sA}{1 + sA} \right). \tag{19}$$

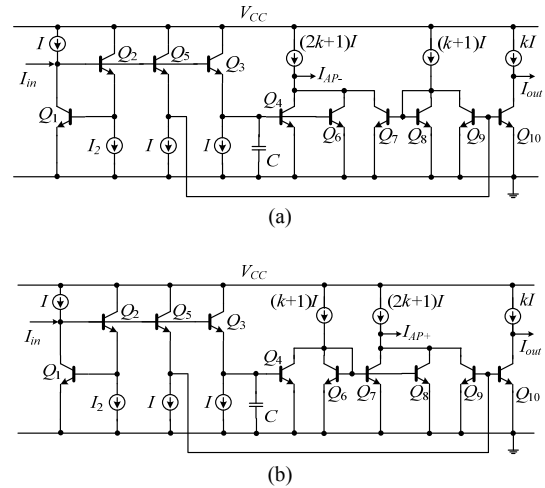


Fig. 6. The proposed log-domain first-order AP filter: (a) Inverting, (b) Non-inverting.

Using methodology in Fig. 5(a) to realize the circuit then it can be depicted as Fig. 6(a). Transistors Q_1 , Q_2 , Q_3 , Q_4 and Q_6 are realized to inverting LP filter with gain = 2. At the same time, transistors Q_1 , Q_2 , Q_5 and Q_9 are realized to inverting current gain ($-k$) then its output connects to the other inverting function which is provided by current mirror Q_7 and Q_8 . Non-inverting current gain is achieved by the collector output of Q_7 . Summing the current outputs of LP filter with gain=2 (Q_4 and Q_6) and non-inverting current

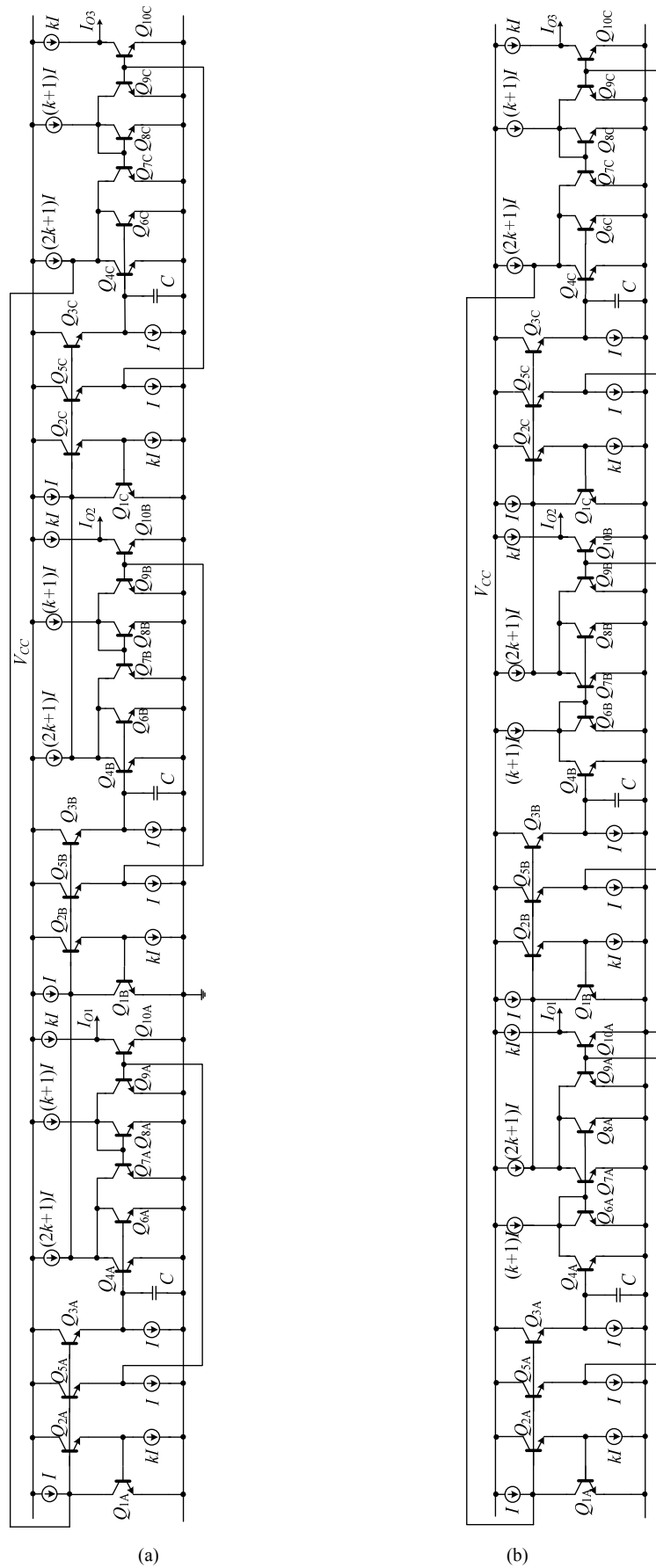


Fig. 7. Log-domain allpass-based MSO structures: (a) odd $n = 3$, (b) odd/even $n = 3$.

gain (Q_7), the inverting AP filter is achieved. The current transfer functions can be written as

$$\frac{I_{out}}{I_{in}} = -k, \quad (20)$$

$$\frac{I_{AP-}}{I_{in}} = -k \left(\frac{1-sCV_T/I}{1+sCV_T/I} \right). \quad (21)$$

Using methodology in Fig. 5(b) to realize the circuit then it can be depicted as Fig. 6(b). Using similar concept to Fig. 6(b), the current gain transfer function is the same as (20), but the current output of AP function (Q_7 , Q_8 and Q_9) becomes non-inverting transfer function as

$$\frac{I_{AP+}}{I_{in}} = k \left(\frac{1-sCV_T/I}{1+sCV_T/I} \right). \quad (22)$$

Considering (21) and (22) with AP function in section 2.1, $A = CV_T/I$ and $k = I_2/I$ for inverting and non-inverting AP filters. The frequency response and stage gain can be independently tuned through bias current.

3. Current-mode Log-domain MSO

A three-phase MSO concept based on Fig. 1 and 2 is implemented to confirm the theory shown in Fig. 7. The first AP-based MSO is realized by cascading three inverting AP filters. The second AP-based MSO is also realized by cascading two non-inverting and one inverting AP filters.

From Fig. 7(a), loop-gain of this circuit is actually adjusted to unity for obtaining the oscillation condition. Unity stage gain ($k = 1$) is defined for obtaining the oscillation condition. The bias currents are assigned to $k = 1$ by setting $kI = I$. Each negative stage (AP1-AP3) provides high output impedance that drives to the succeeding stage. The inverting first-order AP filter sections are given by

$$\frac{I_{out}}{I_{in}} = -k \left(\frac{1-sCV_T/I}{1+sCV_T/I} \right). \quad (23)$$

The result in three cascaded AP filter yields

$$H(s) = \left[- \left(\frac{1-s(CV_T/I)}{1+s(CV_T/I)} \right) \right]^3. \quad (24)$$

From (5), the frequency of oscillation gives

$$\omega_0 = \frac{A}{\sqrt{3}} = \frac{I}{\sqrt{3}CV_T}. \quad (25)$$

From Fig. 7(b), three-phase MSO based on Fig. 2 is also implemented to confirm the theory. The non-inverting first-order AP filter sections are given by

$$\frac{I_{out}}{I_{in}} = k \left(\frac{1-sCV_T/I}{1+sCV_T/I} \right). \quad (26)$$

The result in three cascading two non-inverting and one inverting AP filters yields

$$H(s) = - \left[\left(\frac{1-s(CV_T/I)}{1+s(CV_T/I)} \right)^3 \right]. \quad (27)$$

From (5), the frequency of oscillation gives

$$\omega_0 = \frac{A}{\sqrt{3}} = \frac{I}{\sqrt{3}CV_T}. \quad (28)$$

4. Influence of Non-idealities

Log-domain filter suffers from transistor non-idealities effect. The study of non-ideal log-domain filters is complicated by the fact that the non-linear logarithmic-exponential operations inherent the circuit result in transcendental equations. This qualitative analysis shows that the transistor non-idealities including the parasitic resistances and parasitic capacitances are the sources of error within log-domain circuits. This paper derives equations describing the non-ideal characteristics of log-domain circuit as a consequence of the deviations in non-ideal parameters. This section shows the effects of transistor parasitic in Fig. 8 based on a small-signal model using transconductance $g_m = I_C/V_T$, base-emitter resistance (r_π), base-emitter capacitance (C_π), and base-collector capacitance (C_μ). We assume that the other parasitic capacitances are very small and the impedance of the collector-emitter (r_{ce}) is high. Physical parameters such as area mismatch and early voltage are also discussed.

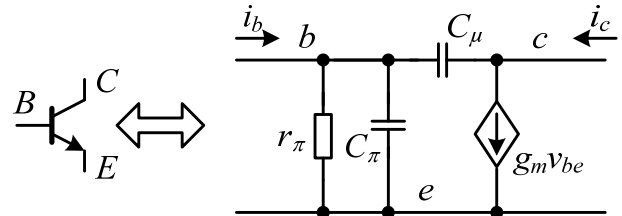


Fig. 8. Simple small signal of BJT transistor.

Taking the model in Fig. 8 into log-domain AP filter in Fig. 6, the input and output resistances are obtained around $1/g_{m1}$ and $r_o/3$, respectively. As resulting of input and output resistances, the circuit is agreed well in current-mode approach.

4.1 Parasitic Capacitance (C_π and C_μ)

Parasitic base-emitter capacitance (C_π) is also a major limitation of translinear circuit accuracy, particularly in high-frequencies. Using the small-signal model of the bipolar transistor with parasitic capacitances, the C_π that affects inverting and non-inverting all-pass filter transfer functions can, respectively, be approximated to (29) and (30). Similarly, parasitic base-collector capacitance (C_μ) is

also a major limitation to translinear circuit accuracy. The effect of the base-collector capacitance that affects invert-

ing and non-inverting all-pass filter transfer functions are given by (31) and (32), respectively.

$$\frac{i_{ap-}(s)}{i_{in}(s)} \approx \frac{g_{m2}g_{m3}(g_{m9} - 2g_{m4}) - s[2g_{m3}g_{m4}(C_{\pi1} + C_{\pi2} + C_{\pi9}) - g_{m2}g_{m9}(C_{\pi3} + C_{\pi4} + C_1) + 2C_{\pi3}g_{m2}g_{m4} - C_{\pi2}g_{m3}g_{m9}]}{g_{m1}g_{m2}g_{m3} + s[g_{m1}g_{m2}(C_{\pi3} + C_{\pi4} + C_1) + g_{m1}g_{m3}C_{\pi2}]}, \quad (29)$$

$$\frac{i_{ap+}(s)}{i_{in}(s)} \approx \frac{g_{m2}g_{m3}(2g_{m4} - g_{m9}) + s[2g_{m3}g_{m4}(C_{\pi1} + C_{\pi2} + C_{\pi9}) - g_{m2}g_{m9}(C_{\pi3} + C_{\pi4} + C_1) + 2g_{m2}g_{m4}C_{\pi3} - g_{m3}g_{m9}C_{\pi2}]}{g_{m1}g_{m2}g_{m3} + s[(C_{\pi3} + C_{\pi4} + C_1)g_{m1}g_{m2} + C_{\pi2}g_{m1}g_{m3}]}, \quad (30)$$

$$\frac{i_{ap-}(s)}{i_{in}(s)} \approx \frac{g_{m2}g_{m3}(g_{m9} - 2g_{m4}) + s[C_{\mu1}g_{m3}g_{m9} - 2g_{m3}g_{m4}(C_{\mu1} + C_{\mu9}) + g_{m2}g_{m9}(C_1 + C_{\mu4}) + g_{m2}g_{m3}(2C_{\mu4} - C_{\mu9})]}{g_{m1}g_{m2}g_{m3} + s[g_{m1}g_{m2}(C_{\mu4} + C_1) + g_{m2}g_{m3}(C_{\mu2} + C_{\mu3}) + g_{m1}g_{m3}C_{\mu1}]}, \quad (31)$$

$$\frac{i_{ap+}(s)}{i_{in}(s)} \approx \frac{g_{m2}g_{m3}(2g_{m4} - g_{m9}) - s[C_{\mu1}g_{m3}g_{m9} - 2g_{m3}g_{m4}(C_{\mu1} + C_{\mu9}) + g_{m2}g_{m9}(C_1 + C_{\mu4}) + g_{m2}g_{m3}(2C_{\mu4} - C_{\mu9})]}{g_{m1}g_{m2}g_{m3} + s[g_{m1}g_{m2}(C_{\mu4} + C_1) + g_{m2}g_{m3}(C_{\mu2} + C_{\mu3}) + g_{m1}g_{m3}C_{\mu1}]}. \quad (32)$$

Assuming that the transconductances of the transistors are matched, the transfer function becomes (33)-(36).

$$\frac{i_{ap-}(s)}{i_{in}(s)} \approx \frac{s \frac{[(C_1 + C_{\pi4} - C_{\pi2} - C_{\pi3}) - 2(C_{\pi1} + C_{\pi9})]}{g_m} - 1}{s \frac{(C + C_{\pi3} + C_{\pi4} + C_{\pi2})}{g_m} + 1}, \quad (33)$$

$$\frac{i_{ap+}(s)}{i_{in}(s)} \approx \frac{-s \frac{[(C_1 + C_{\pi4} - C_{\pi2} - C_{\pi3}) - 2(C_{\pi1} + C_{\pi9})]}{g_m} + 1}{s \frac{(C + C_{\pi3} + C_{\pi4} + C_{\pi2})}{g_m} + 1}, \quad (34)$$

$$\frac{i_{ap-}(s)}{i_{in}(s)} \approx \frac{s \frac{(C_1 + C_{\mu4} + 2C_{\mu4} - C_{\mu1} - 3C_{\mu9})}{g_m} - 1}{s \frac{(C + C_{\mu4} + C_{\mu2} + C_{\mu3} + C_{\mu1})}{g_m} + 1}, \quad (35)$$

$$\frac{i_{ap+}(s)}{i_{in}(s)} \approx \frac{-s \frac{(C_1 + C_{\mu4} + 2C_{\mu4} - C_{\mu1} - 3C_{\mu9})}{g_m} + 1}{s \frac{(C + C_{\mu4} + C_{\mu2} + C_{\mu3} + C_{\mu1})}{g_m} + 1}. \quad (36)$$

From (33)-(36), it can be seen that parasitic capacitances C_{π} and C_{μ} produce a small deviation in the frequency response of all-pass filter. Since the natural frequency has been $\omega_0 = g_m/C = I/CV_T$, high frequency operation can be realized by increasing the bias current or reducing the capacitance. To maintain the low-power, the bias currents are kept at a lower level and the integrating capacitance is increased. To prevent significant distortion, the selected capacitance C should be

$$C \gg 4C_{\pi i} + 3C_{\mu i}. \quad (37)$$

4.2 Area Mismatches

Emitter area mismatches cause variations in the saturation current (I_S) between transistors. Taking into account

the emitter area, equation (15) can be rewritten as

$$\lambda k I_i = I_o + \frac{C_1 \dot{I}_o V_T}{I} \quad (38)$$

$$\text{where } \lambda = \frac{I_{S3}I_{S4}}{I_{S1}I_{S2}} = \frac{A_3A_4}{A_1A_2}.$$

From (38), it is clear that area mismatches introduce only a change in the proportionality constant or DC gain of the low-pass filter without affecting the linearity or the time constant of the circuit. The gain error can be easily compensated by adjusting one of the DC bias currents.

4.3 Early Effect

Early effect (base-width modulation) causes the collector current error by the collector-emitter and base-collector voltages. Considering the variation of collector-emitter voltage, the collector current can be written as $I_c = (1 + V_{ce}/V_A)I_S \exp(V_{be}/V_T)$, where V_A is the forward-biased early voltage. An analysis of the integrator shows the early effect with a scalar error to the DC gain of the circuit as in case of area mismatches. Since V_{ce} has been signal-dependent, the device base-width modulation also introduces distortion. Since the voltage swings in the current-mode companding circuits have been very low ($\delta V_{be}S$), the early effect is not a major source of distortion.

4.4 Parasitic Resistance (r_{π})

Parasitic base-emitter resistance (r_{π}) is a major limitation of the translinear circuit accuracy in high-frequencies. Base-emitter resistance has generally been identified as the most problematic error sources in lower frequencies [28] and also produced noise temperature.

From the small-signal model of bipolar transistor, when the parasitic capacitances are neglected, the r_{π} that affects inverting and non-inverting all-pass filter transfer functions are, respectively, described in (39) and (40).

$$\frac{i_{ap-}(s)}{i_{in}(s)} \approx \frac{-2r_{\pi 1}r_{\pi 2}r_{\pi 3}r_{\pi 4}r_{\pi 7}g_{m2}g_{m3}g_{m4} + r_{\pi 1}r_{\pi 2}r_{\pi 3}r_{\pi 4}r_{\pi 7}g_{m2}g_{m3}g_{m7} + s(r_{\pi 1}r_{\pi 2}r_{\pi 3}r_{\pi 4}r_{\pi 7}g_{m2}g_{m7}C_1)}{r_{\pi 1}r_{\pi 2}r_{\pi 3}r_{\pi 4}r_{\pi 7}g_{m1}g_{m2}g_{m3} + s(r_{\pi 1}r_{\pi 2}r_{\pi 3}r_{\pi 4}r_{\pi 7}g_{m1}g_{m2}C_1)}, \quad (39)$$

$$\frac{i_{ap+}(s)}{i_{in}(s)} \approx \frac{2r_{\pi 1}r_{\pi 2}r_{\pi 3}r_{\pi 4}r_{\pi 9}g_{m2}g_{m3}g_{m4} - r_{\pi 1}r_{\pi 2}r_{\pi 3}r_{\pi 4}r_{\pi 9}g_{m2}g_{m3}g_{m9} - s(r_{\pi 1}r_{\pi 2}r_{\pi 3}r_{\pi 4}r_{\pi 9}g_{m2}g_{m9}C_1)}{r_{\pi 1}r_{\pi 2}r_{\pi 3}r_{\pi 4}r_{\pi 9}g_{m1}g_{m2}g_{m3} + s(r_{\pi 1}r_{\pi 2}r_{\pi 3}r_{\pi 4}r_{\pi 9}g_{m1}g_{m2}C_1)}. \quad (40)$$

Equations (39) and (40) can be simplified and rewritten as

$$\frac{i_{ap-}(s)}{i_{in}(s)} \approx \frac{-2g_{m3}g_{m4} + g_{m3}g_{m7} + s(g_{m7}C_1)}{g_{m1}g_{m3} + s(g_{m1}C_1)}, \quad (41)$$

$$\frac{i_{ap+}(s)}{i_{in}(s)} \approx \frac{2g_{m3}g_{m4} - g_{m3}g_{m9} - s(g_{m9}C_1)}{g_{m1}g_{m3} + s(g_{m1}C_1)}. \quad (42)$$

From (41) and (42), it can be seen that both types of all-pass filter have no effects from the parasitic resistance (r_{π}). In other words, noise temperature of the circuit which is produced by parasitic resistances has been reduced.

4.5 Errors of Bias Currents

The proposed log-domain filter employs bias currents which are provided by positive and negative current sources. The positive (I_P) and negative (I_N) current sources are respectively replaced by positive and negative current mirrors in Fig. 9. The transconductances of transistors are controlled by the particular bias currents. Positive and negative current mirror errors which affect the filter performances are considered. Based on the configuration of Fig. 9, the positive and negative bias currents are given by $I_P = \alpha_P I$ and $I_N = \alpha_N I$, where α_P and α_N represent the current gain of positive and negative current mirrors, respectively. It can be seen that transconductances $g_{m1} = g_{m4} = g_{m7} = g_{m9} = I_P/V_T$ and $g_{m3} = I_N/V_T$, then (41) and (42) become

$$\frac{i_{ap-}(s)}{i_{in}(s)} \approx \frac{-(I_N I_P / V_T^2) + s(C_1 I_P / V_T)}{(I_N I_P / V_T^2) + s(C_1 I_P / V_T)}, \quad (43)$$

$$\frac{i_{ap+}(s)}{i_{in}(s)} \approx \frac{(I_N I_P / V_T^2) - s(C_1 I_P / V_T)}{(I_N I_P / V_T^2) + s(C_1 I_P / V_T)}. \quad (44)$$

It can be seen that the current gain of current mirrors affect AP filter configuration. The pole (ω_{0p}) and zero (ω_{0z}) frequencies can be rewritten as

$$\omega_{0p} = \omega_{0z} = \frac{\alpha_N I}{V_T C_1}. \quad (45)$$

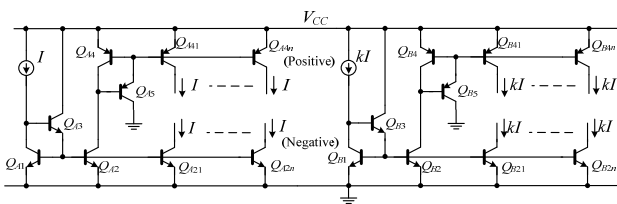


Fig. 9. Biasing circuit of proposed all-pass based MSO.

As we see from (45), there is a slight deviation in the pole of zero frequency due to the mismatch in bias currents. The error can be eliminated by using the accurate bias currents as cascode current mirrors

5. Simulation Results

In order to verify the operation of MSO topology in Fig. 7, power supply voltage is assigned to $V_{CC} = 2.5$ V, current-gain $k = 1.047$ and the bias current I is varied from $0.01 \mu\text{A}$ to $1,000 \mu\text{A}$. To prevent the parasitic effects of the filter, capacitors should be much larger than $4C_{\pi} + 3C_{\mu}$ (around 0.5 pF) by assigning $C_1 = C_2 = 50$ pF. According to section 2, the low-frequency stage gain of each all-pass filter must be unity based on identical current bias I . The NPN high-speed bipolar technology (HSB2) provided by ST Microelectronics [25] is used in the simulations and listed in Tab. 1(a). The bias currents realized by using the current mirrors as shown in Fig. 9 are provided by NPN and PNP (HFA3128 transistor arrays) models in Tab. 1(a) and (b), respectively.

```

.MODEL C12TYP NPN
+ (IS=7.40E-018 BF=1.00E+002 BR=1.00E+000 NF=1.00E+000
+ NR=1.00E+000 TF=6.00E-012 TR=1.00E-008 XTF=1.00E+001
+ VTF=1.50E+000 ITF=2.30E-002 PTF=3.75E+001 VAF=4.50E+001
+ VAR=3.00E+000 IKF=3.10E-002 IKR=3.80E-003 ISE=2.80E-016
+ NE=2.00E+000 ISC=1.50E-016 NC=1.50E+000 RE=5.26E+000
+ RB=5.58E+001 IRB=0.00E+000 RBM=1.55E+001 RC=8.09E+001
+ CJE=3.21E-014 VJE=1.05E+000 MJE=1.60E-001 CJC=2.37E-014
+ VJC=8.60E-001 MJC=3.40E-001 XCJC=2.30E-001 CJS=1.95E-014
+ VJS=8.20E-001 MJS=3.20E-001 EG=1.17E+000 XTB=1.70E+000
+ XTI=3.00E+000 KF=0.00E+000 AF=1.00E+000 FC=5.00E-001)
    
```

(a) NPN-HSB2 provided by ST Microelectronics

```

.model HFA3128 PNP
+ (IS=1.027E-16 XTI=3.000E+00 EG=1.110E+00 VAF=3.000E+01
+ VAR=4.500E+00 BF=5.228E+01 ISE=9.398E-20 NE=1.400E+00
+ IKF=5.412E-02 XTB=0.000E+00 BR=7.000E+00 ISC=1.027E-14
+ NC=1.800E+00 IKR=5.412E-02 RC=3.420E+01 CJC=4.951E-13
+ MJC=3.000E-01 VJC=1.230E+00 FC=5.000E-01 CJE=2.927E-13
+ MJE=5.700E-01 VJE=8.800E-01 TR=4.000E-09 TF=20.05E-12
+ ITF=2.001E-02 XTF=1.534E+00 VTF=1.800E+00 PTF=0.000E+00
+ XCJC=9.000E-01 CJS=1.150E-13 VJS=7.500E-01 MJS=0.000E+00
+ RE=1.848E+00 RB=3)
    
```

(b) PNP-HFA3128 provided by Intersil.

Tab. 1. Bipolar model parameter of used for SPICE simulation.

Fig. 10 depicts the magnitude response of log-domain LP filter. The controlled current-gain is obtained by adjusting the particular bias current (kI). Frequency response has no effects from the current-gain. Fig. 11 illustrates the current-gain with $40 \mu\text{A}$ -p sinusoidal input waveform and

the current outputs that provided by adjustable current-gain based on varied bias currents.

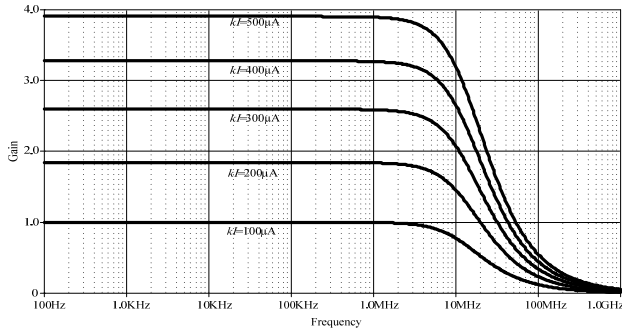


Fig. 10. Magnitude response of LP filter with gain tunability when $I = 1,000 \mu\text{A}$ and $C = 50 \text{ pF}$.

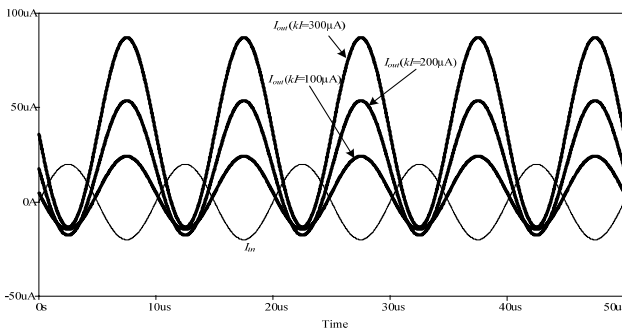


Fig. 11. Waveform output of LP filter by varying kI when $I = 100 \mu\text{A}$ and $C = 50 \text{ pF}$.

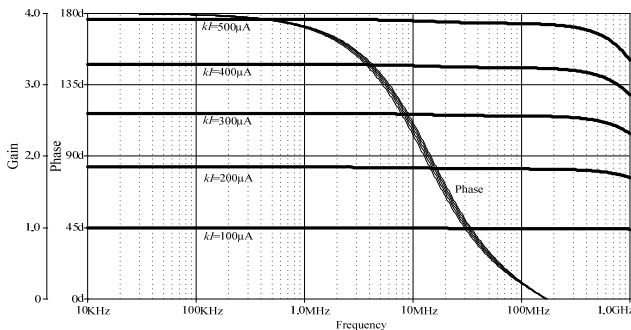


Fig. 12. Magnitude and phase response of AP filter with gain tunability when $I = 1,000 \mu\text{A}$ and $C = 50 \text{ pF}$.

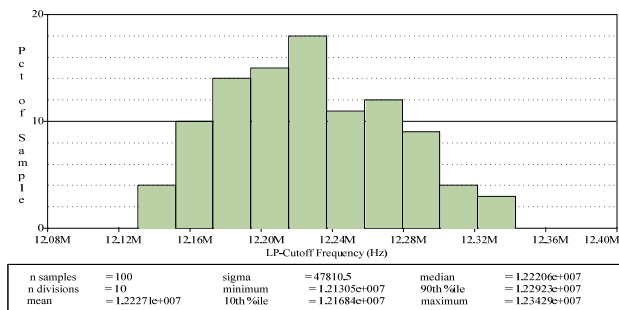


Fig. 13. Monte Carlo simulation of log-domain LP filter when transistors have 20% deviation of β .

Fig. 12 depicts the magnitude and phase responses of log-domain AP filter. The controlled current-gain is ob-

tained by adjusting the particular bias current (kI). Frequency response has very small effect from the current-gain.

Fig. 13 exhibits the performance analysis by using Monte Carlo simulation. Hundred of samples are run for verifying the frequency response. The finite beta of transistors ($\beta = g_m r_\pi$) due to process by 20% deviation is slightly affected to the cut-off frequency of log-domain LP filter. It is also in agreement with section 4.4 (circuit has no influence from r_π).

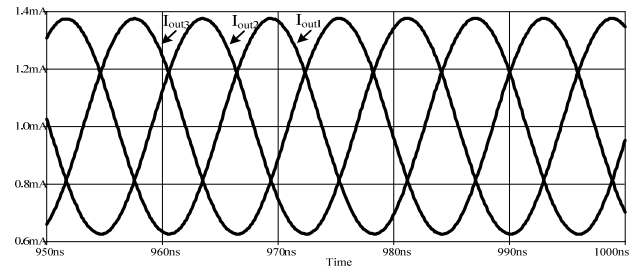


Fig. 14. Sinusoidal outputs (Odd Structure) when $I = 1,000 \mu\text{A}$ and $C = 50 \text{ pF}$.

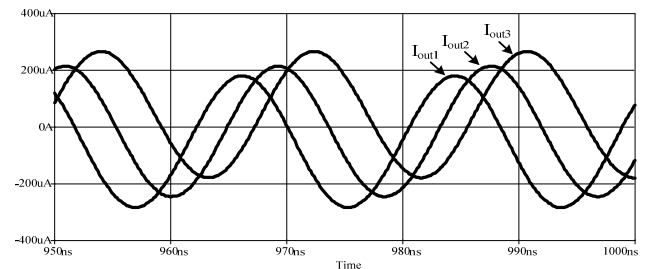


Fig. 15. Sinusoidal outputs (odd/even structure) when $I = 1,000 \mu\text{A}$ and $C = 50 \text{ pF}$.

The odd and odd/even three phase current sinusoidal signal outputs are illustrated in Fig. 14 and 15, respectively. The simulated oscillation frequencies of both structures provide, respectively, 56.67 MHz and 54.44 MHz, while the theoretically value is 70.68 MHz. Simulations of power consumption are obtained around 100 mW.

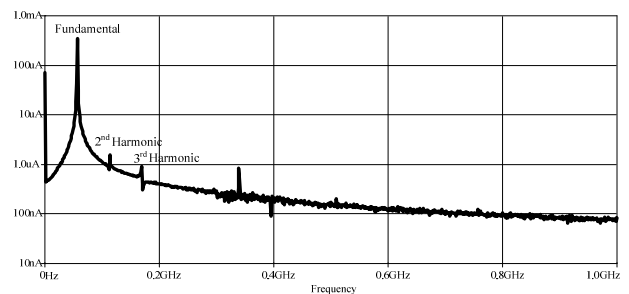


Fig. 16. Spectrum of signal in Fig. 14.

The frequency spectrum of the sinusoidal signal output of Fig. 14 is shown in Fig. 16. The 2nd and 3rd harmonic components are obtained around 1.56 μA , 941.77 nA, respectively, while the amplitude of the fundamental component (56.67 MHz) is around 346 μA ; hence, the THD is obtained around 0.52%.

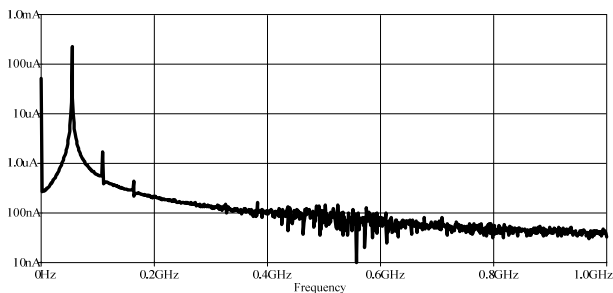


Fig. 17. Spectrum of signal in Fig. 15.

The frequency spectrum of the sinusoidal signal output of Fig. 15 is shown in Fig. 17. The 2nd and 3rd harmonic components are obtained around 1.67 μA , 441.86 nA, respectively, while the amplitude of the fundamental component (54.44 MHz) is around 230.53 μA ; hence, the THD is obtained around 0.75%.

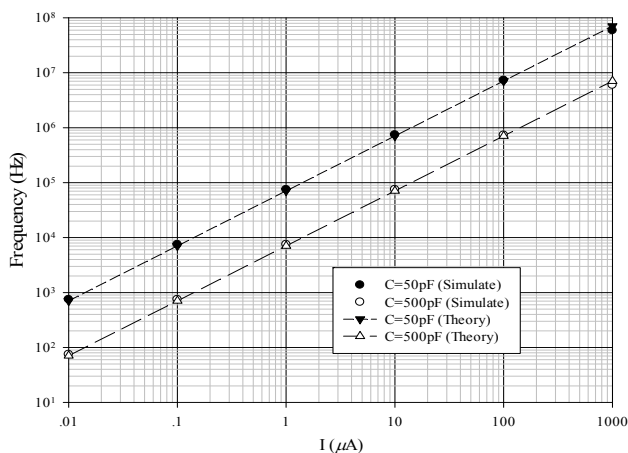


Fig. 18. Tunable frequency of oscillation by using various bias currents.

The tunable frequency of oscillation of AP filter based MSO can be accommodated by varying the current bias (I) from 0.01 μA to 1,000 μA with different capacitor values. A comparison between simulation and theoretical results are shown in Fig. 18. A wide-range of frequency of oscillation (from 750 Hz to 56.67 MHz) can be obtained based on $C_1 = C_2 = 50$ pF. PSpice simulation results agree well with the theory.

6. Conclusion

A novel low-voltage current-mode MSO based on log-domain AP filter has been presented. Inverting and non-inverting log-domain AP filters are realized based on LP filter. Both types of AP filters are realized by 10 transistors, a grounded capacitor and 7 bias currents. Due to log-domain concepts, inverting and non-inverting AP filter can provide the high performance feature, such as high frequency operation and linear wide range tuning. Two structures of MSO (odd and odd/even) can be realized based on cascading log-domain inverting and non-inverting AP filters. The proposed three phases MSOs consist of 30

transistors, 21 bias current sources and 3 grounded capacitors. Multiphase sinusoidal output currents with high output impedance are produced based on a 2.5 V power supply. A wide-range of tunable frequency response (from 750 Hz to 56.67 MHz) can be obtained by varying I_B from 0.01 μA to 1,000 μA . THD at frequency 56.67 MHz is obtained around 0.52%. Power consumption at 1,000 μA is obtained around 100 mW.

References

- [1] ADAMS, R. W. Filtering in the log domain. In 63rd AES Conv., Los Angeles (CA), May 1979, preprint 1470.
- [2] FREY, D. R. Log-domain filtering: An approach to current-mode filtering. *Proc. IEE, part-G*, 1993, vol. 140, no. 6, p. 406–416.
- [3] FREY, D. R. Exponential state-space filters: a generic current mode design strategy. *IEEE Trans Circuits Systems-I*, 1996, vol. 43, p. 34–42.
- [4] SEEVINCK, E. Companding current-mode integrator: A new circuit principle for continuous-time monolithic filters. *Electron. Lett.*, 1990, vol. 26, no. 24, p. 2046–2047.
- [5] TSIVIDIS, Y. On linear integrators and differentiators using instantaneous companding. *IEEE Trans. Circuits Syst. II*, Aug.1995, vol. 42, p. 561–564.
- [6] TSIVIDIS, Y. General approach to signal processors employing companding. *Electron. Lett.*, 1995, vol. 31, no. 18, p. 1549–1550.
- [7] FREY, D. R., TSIVIDIS, Y. Syllabically companding log domain filter using dynamic biasing. *Electron. Lett.*, 1997, vol. 33, no. 18, p. 1506–1507.
- [8] FREY, D. R. A 3.3 V electronically tuneable active filter useable to beyond 1 GHz. In *Proc. IEEE Int. Symp. Circuits Syst. (ISCAS'94)*. London (U.K.), 1994, vol. 5, p. 493–496.
- [9] FREY, D. R. Log domain filtering for RF applications. *IEEE J. Solid-State Circuits*, Oct. 1996, vol. 31, p. 1468–1475.
- [10] FREY D. R. An adaptive analog notch filter using log-filtering. In *Proc. IEEE Int. Symp. Circuits Syst. (ISCAS'96)*. Atlanta (GA), 1996, vol. 1, p. 297–300.
- [11] YANG, F., ENZ, C., RUYMBEKE, G. Design of low-power and low voltage log-domain filters. In *Proc. IEEE Int. Symp. Circuits Syst. (ISCAS'96)*. Atlanta (GA), 1996, vol. 1, p. 117–120.
- [12] DRAKAKIS, E. M., PAYNE A. J., TOUMAZOU, C. Log-domain filtering and the Bernoulli cell. *IEEE Trans. Circuits Syst. I*, May 1999, vol. 46, no. 5, p. 559–571.
- [13] EL-GAMAL, M. N., ROBERTS, G. W. A 1.2-V n-p-n-only integrator for log-domain filtering. *IEEE Trans. Circuits Syst. II*, Apr. 2002, vol. 49, p. 257–265.
- [14] DRAKAKIS, E. M., PAYNE, A. J., TOUMAZOU, C. Log-domain state-space: A systematic transistor level approach for log-domain filtering. *IEEE Trans. Circuits Syst. II*, Mar. 1999, vol. 46, p. 290 to 305.
- [15] PYTHON, D., ENZ, C. A micropower class-AB CMOS log-domain filter for DECT applications. *IEEE J. Solid-State Circuits*, July 2001, vol. 36, no. 7, p. 1067–1075.
- [16] WU, D., LIU, S., HWANG, Y., WU, Y. Multiphase sinusoidal oscillator using second-generation current conveyors. *International Journal of Electronics*, 1995, vol. 78, p. 645–651.

- [17] ABUELMA'ATTI, M. T., AL-QAHTANI, M. A. A new current-controlled multiphase sinusoidal oscillator using translinear current conveyors. *IEEE Transactions on Circuits and Systems-II*, 1998, vol. 45, no. 7, p. 881-885.
- [18] PROMMEE, P., DEJHAN, K. An integrable electronic-controlled quadrature sinusoidal oscillator using CMOS operational transconductance amplifier. *International Journal of Electronics*, 2002, vol. 89, no. 5, p. 365-379.
- [19] GIFT, S. J. G. The application of AP filters in the design of multiphase sinusoidal systems. *Micro-electronics Journal*, 2000, vol. 31, p. 9-13.
- [20] TANGSRIRAT, W., TANJAROEN, W., PUKKALANUN, T. Current-mode multiphase sinusoidal oscillator using CDTA-based allpass sections. *Int. J. Electron. Commun. (AEU)*, 2009, vol. 63, p. 616 - 622.
- [21] JAIKLA, W., PROMMEE, P. Electronically tunable current-mode multiphase sinusoidal oscillator employing CCCDTA-based allpass filters with only grounded passive elements. *Radioengineering*, 2011, vol. 20, no. 3, p. 594-599.
- [22] PSYCHALINOS, C., SOULIOTIS, G. A log-domain multiphase sinusoidal oscillator. *AEU - International Journal of Electronics and Communications*, 2008, vol. 62, no. 8, p. 622-626.
- [23] SERDIJN, W. A., MULDER, J., KOUWENHOVEN, M. H. L., VAN ROERMUND, A. H. M. A low-voltage translinear second-order quadrature oscillator. In *Proc. IEEE Int. Symp. Circuits Syst (ISCAS'99)*. Orlando (Florida, USA), 1999, vol.2, p. 701-704.
- [24] PROMMEE, P., SRA-IUM, N., DEJHAN, K. High-frequency log-domain current-mode multiphase sinusoidal oscillator. *IET Circuits Devices Syst.*, Sep. 2010, vol. 4, no. 5, p. 440-448.
- [25] PROMMEE, P., PRAPAKORN, N., SWAMY, M. N. S. Log-domain current-mode quadrature sinusoidal oscillator. *Radioengineering*, 2011, vol. 20, no. 3, p. 600-607.
- [26] PROMMEE, P., SOMDUNYAKANOK, M. Log-domain all-pass based multiphase sinusoidal oscillator. In *Proc. of IEEE TSP2012*. Prague (Czech Republic), July 3-4, 2012, p. 355 - 358.
- [27] GILBERT, B. Translinear circuits: an historical overview. *Analog Integrated Circuits and Signal Processing*, Mar. 1996, vol. 9, no. 2, p. 95-118.
- [28] LEUNG, V. W., ROBERTS, G. W. Effects of transistor nonidealities on high-order log-domain ladder filter frequency responses. *IEEE Trans. Circuits Syst. II*, 2000, vol. 47, no. 5, p. 373-387.

About Authors ...

Pipat PROMMEE received his B. Ind. Tech. degree in Telecommunications, M.Eng. and D.Eng. in Electrical Engineering from Faculty of Engineering, King Mongkut's Institute of Technology Ladkrabang (KMITL), Bangkok, Thailand in 1992, 1995 and 2002, respectively. He was a senior engineer of CAT telecom pcl. between 1992 and 2003. Since 2003, he has been a faculty member of KMITL. He is currently an associate professor at the Department of Telecommunications Engineering at KMITL. He is author or co-author of more than 60 publications in journals and proceedings of international conferences. His research interests are focusing in Analog Signal Processing, Analog Filter Design and CMOS Analog Integrated Circuit Design. He is a member of IEEE, USA.

Natapong WONGPROMMOON received B.Eng. and M.Eng. degrees in Telecommunications Engineering from Faculty of Engineering, King Mongkut's Institute of Technology Ladkrabang (KMITL), Bangkok, Thailand in 2006, and 2011, respectively, and M.Business in Enterprise Resources Planning (ERP) from University of Western Sydney (UWS), Sydney, Australia in 2007. He was an Application Consultant at Metro systems PCL. since 2007-2009 and a Business Consultant at Business Application Co., Ltd. between 2009 and 2010. Since 2010, he has been a Solution Architect at G-ABLE Co., Ltd. He is presently working toward his D.Eng. in Electrical Engineering at KMITL. His research interests are focusing in analog filter design and analog signal processing.